# Dynamics Learning-Based Fault Isolation for A Soft Trunk Robot

Jingting Zhang, Xiaotian Chen, Emadodin Jandaghi, Wei Zeng, Mingxi Zhou, Chengzhi Yuan

Abstract—In this paper, we investigate the fault isolation (FI) problem of a soft trunk robot and propose a dynamics learning-based FI approach which is generic and applicable to general types of faults. Specifically, an adaptive radial basis function neural network (RBF NN) based dynamics learning scheme is first developed to achieve accurate identification of the robot's dominant dynamics under different faulty modes, and the learned knowledge is stored and represented by constant RBF NN models. The learned results are then merged by using a novel merging mechanism to construct a bank of global RBF NN models, for capturing the characteristics of the robot's dynamics under each specific faulty mode. Based on these models, a bank of FI observers are designed to develop an important capability of accurately reconstructing the robot's dynamics under various faulty modes. The FI scheme is developed using these FI observers, which monitors the robot's operation status online to provide accurate isolation of faults occurring in the robot. Physical experiments are performed on the soft trunk robot to validate the effectiveness of our proposed approaches.

#### I. Introduction

Soft robots have many desirable mechanical properties, e.g., lightweight, inherent compliance and flexibility, which facilitate safe human-robot interaction and operation in a restrained environment [1]. This has motivated a rapidly-increasing demand for soft robots in industrial, surgical and assistive applications [2]. In these applications, desired safety and reliability of soft robots during online operation are paramount. Fault diagnosis is a critical step, which includes: checking whether/when there is a fault in the robot (i.e., fault detection); determining the location, type, or size of the occurring fault (i.e., fault isolation); and making a response to faults for minimum performance degradation and avoiding dangerous situations [3].

In our previous work [4], the fault detection (FD) problem of soft robots has been successfully tackled using an adaptive dynamics learning-based approach. However, this work has not investigated the fault isolation (FI) of soft robots, which is a more challenging problem. The main technical challenge lies in how to accurately extract the characteristics of the robots' dynamics under different faulty modes [5]. For soft robots, due to their complicated structure and excessive degrees of freedom, they have complex dynamics that are very difficult to model [4]; moreover, due to their inherent

This work was supported in part by the National Science Foundation under Grant CMMI-1929729.

J. Zhang, X. Chen, E. Jandaghi and C. Yuan are with the Department of Mechanical, Industrial and Systems Engineering, University of Rhode Island, Kingston RI, USA (e-mail: jingting\_zhang@uri.edu; xiaotian\_chen@uri.edu; cyuan@uri.edu). W. Zeng is with the School of Mechanical and Electrical Engineering, Longyan University, Longyan, China (e-mail: zw0597@126.com). M. Zhou is with the Graduate School of Oceanography, University of Rhode Island, Narragansett RI, USA (e-mail: mzhou@uri.edu).

compliance and flexibility, they have a wide diversity of dynamic behaviors even under the same operating environment (e.g., the same/similar faulty mode). These features could greatly complicate the extraction of faulty characteristics for soft robots, making the associated FI problem very difficult. Although a few research results have been published in recent years, e.g., [6], [7], [8], [9], there are still many issues yet to be adequately addressed. For example, the FI scheme presented in [6] was developed using an attention-based noise compensation module to handle the robot's vibration behavior under faulty modes, but this approach is limited to lockedmotor faults. Koopman operator was used in [7] to identify the robot's dynamics under different payloads, which cannot be extended to other general types of faults. [8], [9] developed an active FI scheme by imposing the piecewise constantcurvature assumption on the studied robots, which limits their wider applicability to more general soft robots.

In this paper, we will propose an adaptive dynamics learning-based approach for the FI problem in the context of a soft trunk robot. General types of faults will be considered, including component faults (e.g., the robot's air tube is blocked), actuator faults (e.g., the robot's pump motor has a problematic power voltage), and sensor faults (e.g., the robot's sensors deviate from the desired position). Specifically, to extract the characteristics of these faults, in the training phase, we develop an adaptive radial basis function neural network (RBF NN) based dynamics learning scheme to identify the robot's complex nonlinear uncertain dynamics, and the learned knowledge can be obtained and stored in constant RBF NN models [10]. In particular, knowing that the soft robot could have a wide diversity of dynamics under faulty modes, we will train a sufficiently-large number of robot's dynamics under each specific faulty mode, and obtain a bank of local constant NN models to represent the learned knowledge. By merging these local NN models with a novel merging mechanism motivated by [11], a global constant RBF NN model can be constructed to represent the global knowledge of the soft robot's dynamics under the corresponding faulty mode, which can be used to capture the associated faulty characteristics. In the FI phase, a bank of FI observers will be designed using these global NN models, which can develop an important capability of accurately approximating the robot's dynamics under various faulty modes. The FI scheme is then developed based on these FI observers. By online comparing the dynamics of the FI observers and those of the soft robot, the robot's real-time operation mode can be identified, and the type of fault occurring in the robot can be recognized in real time. Physical experiments have been conducted to validate the effectiveness of our proposed







Fig. 1: The soft trunk robot studied in this paper: the robot's prototype (left); the actuators' setup (middle); and the sensors' arrangement (right).

methods.

It should be noted that this paper extends our previous work [4] on the FD problem of soft robots. Several features of our current work distinguished from [4] need to be emphasized. First, we develop a new output-feedback dynamics learning scheme for the soft robot without using a high-gain observer, which could facilitate improving the learning accuracy and FI capability. This advances the scheme of [4] where the dynamics learning process was achieved by using a high-gain observer that could yield large oscillations in the presence of noise and increase the dynamics-learning errors. Furthermore, we propose new FI observers by using a bank of global RBF NN models constructed with a novel merging mechanism, which can more effectively capture the characteristics of the robot's faulty dynamics for FI purpose. This advances our previous work [4] where the associated FD observer was designed without using the merging mechanism.

The main contributions of this paper are: (i) we solve the FI problem of a soft trunk robot by considering general types of faults; (ii) we propose a dynamics learning-based FI scheme for the soft trunk robot by extending our previous work of [4]; and (iii) we perform physical experiments on the soft trunk robot to validate our proposed approaches.

The rest of the paper is organized as follows. Section II includes the problem statement. The adaptive dynamics learning scheme and the FI scheme are presented in Sections III and IV, respectively. Experimental results are given in Section V. Section VI concludes the paper.

## II. PROBLEM STATEMENT

## A. The Soft Trunk Robot

The soft trunk robot studied in this paper is the same as the one in our previous work of [4], as shown in Fig. 1. This robot is pneumatic actuated and composed of three identical segments made of high elasticity silicone rubber. Each segment is able to vertically extend and shrink by pressurizing/depressurizing the inside air. It is actuated by using an air tube to link with two pump motors and one electrical air valve. Five reflective balls are sensors fixed on the robot's top to locate the end-effector. For this soft robot, during its online operation, four general types of faults could occur, including: (i) fault 1: one of the robot's air tubes is blocked; (ii) fault 2: different one of the air tubes is blocked; (iii) fault 3: the power voltage of one of the pump motors raises by 50%; and (iv) fault 4: the reflective balls

deviate from the desired position locating the end-effector. These faults are indexed by  $k \in \mathcal{K} = \{1, 2, 3, 4\}$ , and can be classified as the component faults (i.e., faults 1,2), the actuator fault (i.e., fault 3), and the sensor fault (i.e., fault 4), according to the definitions given in [3].

#### B. Study Objectives

In this paper, our objective is to develop an FI scheme for the soft trunk robot in Fig. 1, and to determine the type of fault  $k \in \mathcal{K}$  that occurs in the robot. The design of our FI scheme will be consisted of: (i) the faulty dynamics learning phase: developing an RBF NN-based learning approach to identify the soft robot's dominant dynamics under different faulty modes, to obtain the learned knowledge for capturing the characteristics of the robot's dynamics under each specific faulty mode; and (ii) the FI phase: developing an FI scheme with the learned knowledge, to real-time monitor the operation status of the soft robot and to provide accurate isolation for the occurring fault.

#### III. FAULTY DYNAMICS LEARNING

This section will present the identification/learning process for the soft robot's dominant dynamics.

#### A. Dynamics Modeling of Soft Robot

We first derive an analytical model to describe the dominant dynamics of the soft robot in Fig. 1, for facilitating the subsequent dynamics learning process. Details are similar to our previous work in [4], and concluded here for completeness of presentation.

Considering the robot in Fig. 1, from [4, Sec. III-B], by using the finite element method, we can discretize the robot's structure into a mesh of finite elements to establish a finite element model. Then, with Newton's second law, we can derive a dynamic model to describe the robot's motion as:

$$M(q)\dot{v} = P(q) - F(q, v) + H(q)^{\top}u,$$
 (1)

where  $q \in \mathbb{R}^{3n}$  is the 3D displacement of each mesh node in the finite element model (with n being the number of the mesh nodes);  $v \in \mathbb{R}^{3n}$  is the velocity; M(q) is the mass matrix; F(q,v) is the internal forces; P(q) is external forces; H(q) contains the direction of actuator's forces; and  $u \in \mathbb{R}^m$  is the amplitude of actuator's forces (with m=3).

Noting that the model (1) is still not suitable for the subsequent learning process due to its high dimensionality, a model-order reduction process will be performed on this model with the proper orthogonal decomposition technique [12]. Specifically, we first rewrite the model (1) as:

$$\dot{x} = f_x(x) + g_x(x)u,\tag{2}$$

with x=[q;v],  $f_x(x)=[v;M(q)^{-1}(P(q)-F(q,v))]$ , and  $g_x(x)=[0;M(q)^{-1}H(q)^{\top}]$ . From [4, Sec. IV-D1], the state  $x\in\mathbb{R}^{6n}$  of (2) can be approximated by a low-order state  $x_r\in\mathbb{R}^6$ , such that  $x_r=U_r^{\top}x$ ,  $x\approx V_rx_r$  with the projectors  $U_r,V_r$  derived according to [4, Eqs. (4)–(6)]. Then, the model (2) can be approximated by a reduced-order model:

$$\dot{x}_r = U_r^{\top} f_x(x_r) + U_r^{\top} g_x(x_r) u = f_r(x_r) + g_r(x_r) u.$$
 (3)

This model can be used to describe the dominant dynamics of the soft robot in Fig. 1. Particularly, the dynamics  $f_r(x_r)$  and  $g_r(x_r)$  are still unknown, and will be identified in the sequel.

#### B. Dynamics Learning with Output Measurement

Identifying the dynamics of (3) requires the measurement of state  $x_r = U_r^\top x$ , which however might not be available in practice for the robot of Fig. 1. In view of this, we first take a simple variable-transformation for the model (3) as follows. Assume that, by appropriately setting sufficient sensors on the robot in Fig. 1, we can obtain a measurement of  $y \in \mathbb{R}^p$  (with p > 6) such that

$$y = Cx \approx CV_r x_r = C_r x_r$$
, and  $x_r = (C_r^{\top} C_r)^{-1} C_r^{\top} y$ , (4)

where C and  $C_r$  are the output matrices for picking out the measurement y respectively from the robot's states x and  $x_r$ ; and the matrix  $C_r$  can be of full rank by appropriately arranging the sensors on the robot, according to [4, Rem. 1]. Based on (4), the model (3) can be transformed into:

$$\dot{y} = C_r f_r((C_r^{\top} C_r)^{-1} C_r^{\top} y) + C_r g_r((C_r^{\top} C_r)^{-1} C_r^{\top} y) u$$
  
=  $f(y) + g(y)u$ . (5)

Thus, the robot's dominant dynamics  $f_r(\cdot)$  and  $g_r(\cdot)$  in (3) can be captured by the dynamics  $f(\cdot)$  and  $g(\cdot)$  in (5). This enables that the robot's dominant dynamics can be identified by directly using the robot's output y, with avoiding using a high-gain observer for state estimation as adopted in [4].

Based on the model (5), by following a similar line of our previous work in [4, Sec. IV-B], we can develop an RBF NN-based adaptive dynamics identifier as follows:

$$\begin{cases} \dot{\hat{y}} = -a(\hat{y} - y) + \hat{W}_{1}^{\top} S_{1}(y) + \hat{W}_{2}^{\top} S_{2}(y) u, \\ \dot{\hat{W}}_{1} = -\Gamma_{1} S_{1}(y) (\hat{y} - y)^{\top} - \Gamma_{1} \sigma_{1} \hat{W}_{1}, \\ \dot{\hat{W}}_{2} = -\Gamma_{2} S_{2}(y) u (\hat{y} - y)^{\top} - \Gamma_{2} \sigma_{2} \hat{W}_{2}, \end{cases}$$
(6)

where y is the robot's output measurement of (4); u is the robot's control input;  $\hat{W}_i$  (i=1,2) is the NN weight;  $S_i(y)$  is an RBF vector; a>0,  $\Gamma_i=\Gamma_i^\top>0$  and  $\sigma_i>0$  are design parameters with  $\sigma_i$  being a small number.

Using the identifier (6) on the model (5), according to [4, Sec. IV-B], it can be deduced that: the accurate identification for the dynamics f(y) and g(y) in (5) can be achieved by the RBF NN models  $\hat{W}_1^{\top}S_1(y)$  and  $\hat{W}_2^{\top}S_2(y)$  in (6), respectively; and the associated NN weights  $\hat{W}_1$  and  $\hat{W}_2$  can converge to a small neighborhood around their constant optimal values. Consequently, through the NN learning process, the learned knowledge of f(y) and g(y) can be obtained and represented by constant RBF NN models as follows

$$f(y) \approx \bar{W}_1^{\top} S_1(y); \quad g(y) \approx \bar{W}_2^{\top} S_2(y),$$
 (7)

where  $\bar{W}_i$  (i=1,2) is the convergent value of  $\hat{W}_i$  in (6), which can be obtained by  $\bar{W}_i = \text{mean}_{t \in [t_1,t_2]} \hat{W}_i(t)$  with  $[t_1,t_2]$  being a time segment after the transient process.

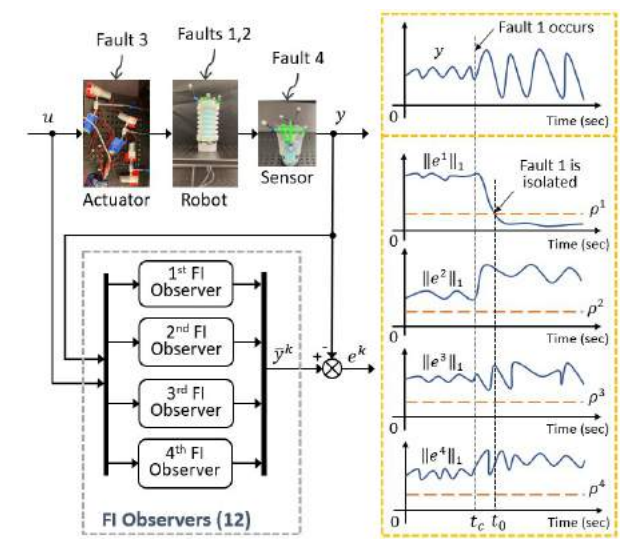


Fig. 2: Schematic diagram of the FI scheme (left) and the FI decision making rule (right), where the fault 1 occurs in the robot at time  $t_c$  and is isolated at time  $t_0$ . u is the control input of the soft robot; y is the robot's output measurement, i.e., the displacement and velocity variables of the robot's endeffector;  $\bar{y}^k$  is the state of k-th FI observer with  $k \in \mathcal{K} = \{1,2,3,4\}; \ \left\|e^k\right\|_1 = \frac{1}{T} \int_{t-T}^t \left|e^k(\tau)\right| d\tau$  (with  $e^k = \bar{y}^k - y$ ) is the FI signal; and  $\rho^k$  is the FI threshold.

### IV. FAULT ISOLATION SCHEME DESIGN

In this section, a bank of FI observers will be designed by using the training results of Section III-B, which are used to online monitor the operation status of the robot in Fig. 1. Our FI scheme will be developed with these FI observers, and its schematic diagram is given in Fig. 2.

#### A. FI Observer Design

Consider that the robot of Fig. 1 is operating under the k-th faulty mode (with  $k \in \mathcal{K}$ ). Following a similar line of (5), the robot's faulty dynamic model can be derived as:

$$\dot{y} = f^k(y) + g^k(y)u, \tag{8}$$

where  $f^k(y)$ ,  $g^k(y)$  include a wide diversity of dynamics of the soft robot under the k-th faulty mode.

For the k-th faulty system of (8), we collect a data set with  $N_k$  number of robot's measurement (y,u). Each measurement data corresponds to a local dynamics  $f^{k_j}(y)$  and  $g^{k_j}(y)$ , i.e.,  $f^k(y) = \cup_{j=1}^{N_k} f^{k_j}(y)$  and  $g^k(y) = \cup_{j=1}^{N_k} g^{k_j}(y)$ . Based on this data set, by implementing the learning scheme of Section III-B, we can obtain the knowledge of these local faulty dynamics by the following constant RBF NN models

$$f^{k_j}(y) \approx \bar{W}_1^{k_j \top} S_1(y); \quad g^{k_j}(y) \approx \bar{W}_2^{k_j \top} S_2(y).$$
 (9)

Then, by using a novel merging mechanism as adopted in [11], we can merge the local NN models of (9) to construct global RBF NN models to represent the knowledge of the global faulty dynamics  $f^k(y)$ ,  $g^k(y)$  in (8), i.e.,

$$f^k(y) \approx \bar{W}_1^{k \top} S_1(y); \quad g^k(y) \approx \bar{W}_2^{k \top} S_2(y),$$
 (10)

with the NN weights given as:

$$\bar{W}_{i}^{k} = \begin{cases} \sum_{j=1}^{N_{k}} \frac{\varrho_{i}^{k_{j}}}{\varrho_{i}^{k}} \bar{W}_{i}^{k_{j}}, & \text{if } \varrho_{i}^{k} \neq 0\\ 0, & \text{if } \varrho_{i}^{k} = 0 \end{cases}$$
(11)

where  $\bar{W}^k_i$  and  $\bar{W}^{k_j}_i$  are the i-th component of  $\bar{W}^k$  and  $\bar{W}^{k_j}$ , respectively (with  $\bar{W}^k = \bar{W}^k_1/\bar{W}^k_2$ , and  $\bar{W}^{k_j} = \bar{W}^{k_j}_1/\bar{W}^{k_j}_2$ );  $\varrho_i^{k_j} = \max_{y=y_{k_i}} S_i(y)$  is the maximum excitation level of the *i*-th node of neurons S(y) in (10) under the robot's  $k_j$ th measurement data  $y_{k_j}$  (with  $S(y) = S_1(y)/S_2(y)$ ); and  $\varrho_i^k = \sum_{j=1}^{N_k} \varrho_i^{k_j}$ . With the global RBF NN models (10), we can design a

bank of FI observers as follows:

$$\dot{\bar{y}}^k = -a(\bar{y}^k - y) + \bar{W}_1^{k \top} S_1(y) + \bar{W}_2^{k \top} S_2(y) u, \ \forall k \in \mathcal{K} \ (12)$$

where (y, u) is the real-time measurement of the robot; and a>0 is a design parameter. For each  $k\in\mathcal{K}$ , by comparing the observer (12) with the system (8), we can obtain the error dynamic system (with  $e^k = \bar{y}^k - y$ ) as follows:

$$\dot{e}^k = -ae^k + (\bar{W}_1^{k\top} S_1 - f^k(y)) + (\bar{W}_2^{k\top} S_2 - g^k(y))u. \tag{13}$$

Noting that the NN models  $\bar{W}_1^{k\top}S_1$ ,  $\bar{W}_2^{k\top}S_2$  can provide an accurate approximation for the dynamics  $f^k(y)$ ,  $g^k(y)$ according to (10), the error signal  $e^{k}$  in (13) can be guaranteed arbitrarily small with a proper parameter a > 0. This verifies that the observer's state  $\bar{y}^k$  of (12) can provide an accurate approximation for the robot's dynamics y under the k-th faulty mode of (8). In particular, such an accurate approximation can be guaranteed only for the robot under the matched k-th faulty mode. The FI observer (12) can thus be used to distinguish the matched k-th faulty mode from other mismatched faulty modes, to facilitate the subsequent development of the FI scheme.

### B. FI Decision Making

Using the designed FI observers (12), we can develop an FI scheme as shown in Fig. 2 by following a similar line of our previous work [5], [13]. Specifically, in the FI process, a bank of FI observers in (12) with  $k \in \mathcal{K} = \{1, 2, 3, 4\}$  are constructed to online monitor the operation status of the robot in Fig. 1. By real-time comparing the robot's measurement y of (4) and observer's states  $\bar{y}^k$  of (12) for all  $k \in \mathcal{K}$ , we can generate the residual signals  $e^k = \bar{y}^k - y$ , and the corresponding FI signals  $\|e^k\|_1 = \frac{1}{T} \int_{t-T}^t \left|e^k(\tau)\right| d\tau$  with T>0 being a design parameter. The FI signal  $\|e^k\|_1$  can be used to characterize the difference between the robot's realtime dynamics and the each k-th faulty dynamics, according to (13). The FI decision making rule is illustrated in Fig. 2, and clarified as follows. Assume that fault 1 occurs in the robot at time  $t_c$ . The robot's real-time dynamics will match the 1-st faulty dynamics, thus their difference (characterized by the FI signal  $\left\|e^1\right\|_1$ ) will decrease and become smaller than a given constant threshold  $\rho^1$  at some time  $t_0$ . Noting that the robot's dynamics does not match other k-th (k = 2, 3, 4) faulty dynamics, their differences (characterized by FI signals  $||e^k||_1$ ) will remain large and

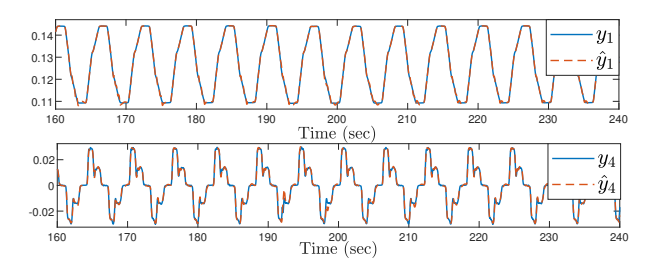


Fig. 3: Approximation performance of the identifier (6) for the soft robot of Fig. 1 under the faulty mode k = 1. y is the displacement and velocity of the robot's end-effector.

larger than their corresponding thresholds  $\rho^k$ . Thus, as seen in Fig. 2, according to the comparison results between the FI signals  $||e^k||_1$  and thresholds  $\rho^k$  in Fig. 2, the occurring fault can be identified as the 1-st type of faults. Such an idea is formalized as follows:

**FI decision making**: Compare the FI signals  $||e^k||_1$  with the corresponding FI thresholds  $\rho^k$  for all  $k \in \mathcal{K}$ . If there exists a finite time  $t_0$  and a unique  $l \in \mathcal{K}$  such that  $e^l \leq$  $\rho^l$  holds for time  $t \geq t_0$ , then, the occurring fault can be identified as the l-th type of faults.

### V. EXPERIMENTAL STUDY ON SOFT ROBOT

In this section, physical experiments will be performed on the soft trunk robot in Fig. 1 to validate our approaches.

## A. Training Phase: Learning of Faulty Dynamics

We enable the robot of Fig. 1 to operate in different faulty modes  $k \in \mathcal{K} = \{1, 2, 3, 4\}$  according to Section II-A. For the training purpose, we collect  $N_k = 20$  number of measurement data (y, u) for each faulty mode, where y is the displacement and velocity variables of the robot's endeffector and u is the robot's control input. Using these data, the dynamics learning process can be implemented according to Section III-B. The learning performance of the identifier (6) for the robot's dynamics under the faulty mode k=1is illustrated in Fig. 3, in which the identifier's state  $\hat{y}$  can provide an accurate approximation for the robot's dynamics y. This verifies the effectiveness of our proposed dynamics learning scheme in Section III-B.

## B. Testing Phase: Isolation of Different Faults

1) Validation of FI Observers: After the training process, we can obtain  $4 \times 20 = 80$  of constant RBF NN models (9) to represent the learned knowledge of the robot's local dynamics under the faulty modes k = 1, 2, 3, 4. By merging these local NN models, we can obtain 4 of global NN models (10) specific to each faulty mode k = 1, 2, 3, 4, and the FI observers can be constructed according to (12). To examine the performance of these observers, we consider that the robot of Fig. 1 operates in 1-st faulty mode, and the approximation performance of the matched 1-st FI observer is illustrated in Fig. 4a. It is shown that the observer's state  $\bar{y}^1$  can provide an accurate approximation for the robot's dynamics y. To further show the advantage of such an FI observer, we compare its

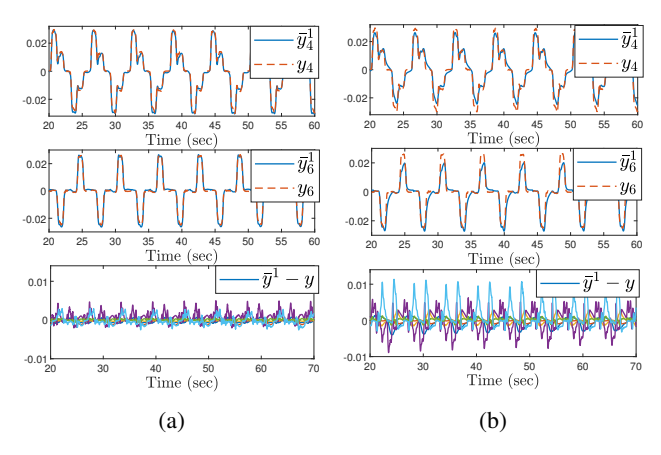


Fig. 4: Approximation performance for the soft robot of Fig. 1 under the faulty mode k=1 using: (a) the proposed observer of (12); and (b) the existing observer of [4]. y is the displacement and velocity of the robot's end-effector.

performance with our previously-proposed observer of [4, Eq. (19)] in Fig. 4. It is seen that compared to the one of [4], the observer (12) can provide a better approximation accuracy for the robot's dynamics. This verifies that advanced over the one of [4], our observer (12) can provide a better approximation performance by using the global knowledge of robot's faulty dynamics, as represented by the global NN models (10).

2) Validation of FI Scheme: Using the constructed FI observers, according to Fig. 2, we can test the performance of our FI approach by using the soft robot of Fig. 1 and the four general types of faults  $k \in \mathcal{K} = \{1, 2, 3, 4\}$  as detailed in Section II-A. We first consider that the fault 2 occurs in the robot, and the FI performance is illustrated in Fig. 5. After the fault's occurrence at time  $t_c = 77.1$  sec, the matched FI signals  $\|e^2\|_1$  will all decrease and become smaller than the corresponding thresholds (i.e., the red dash lines) at time  $t_0 = 80.4$  sec; while the other mismatched FI signals  $\|e^k\|_1$  (k=1,3,4) will remain larger than the corresponding thresholds. Thus, fault k=2 can be isolated at time  $t_0 = 80.4$  sec and the absolute FI time is  $t_0 - t_c = 3.3$ sec. We further consider that the fault 3 occurs in the robot in Fig. 6, in which the FI observers have similar performance, the fault 3 occurs at time  $t_c = 59.9$  sec and is isolated at time  $t_0 = 64.3$  sec, with the absolute FI time being  $t_0 - t_c = 4.4$ sec. As for the faults k = 1 and k = 4, the FI performances are similar to those of faults k = 2 and k = 3, thus are omitted here due to the limited space. By following the same procedure as above, we further test 40 cases for each faulty mode k = 1, 2, 3, 4, and the FI results are summarized in Table I. It verifies that our FI scheme can provide desired FI performance (in terms of the FI success rate and the FI time) for the soft robot with general types of faults.

### VI. CONCLUSION

This paper has investigated the FI problem of a soft trunk robot by considering four general types of faults. Specifically, an adaptive RBF NN-based dynamics learning scheme has been developed to identify the dominant dynamics of the

TABLE I: FI results for the soft robot of Fig. 1 under different faulty modes. FI rate: the ratio of the number of the faults being correctly isolated to the total number of the faults being tested. Absolute FI time: the absolute difference between the fault occurrence time  $t_c$  and the isolated time  $t_0$ . SD: the standard deviation.

Faulty Mode	FI Rate	Absolute FI Time		
		Mean	Max	SD
1	40 / 40	3.44 sec	4.88 sec	0.52 sec
2	40 / 40	3.34 sec	4.94 sec	0.70 sec
3	36 / 40	4.78 sec	6.16 sec	0.48 sec
4	39 / 40	1.28 sec	1.59 sec	0.11 sec

soft robot under different faulty modes, with associated knowledge being obtained and stored in constant RBF NN models. Based on the learned knowledge, a bank of global RBF NN models have been constructed with a novel merging mechanism and used to capture the characteristics of the robot's dynamics under each specific faulty mode. Then, a bank of FI observers have been designed with these global NN models, which can provide an accurate approximation for the robot's dynamics under various faulty modes. The FI scheme has been developed using these FI observers, which can monitor the robot's operation status online and provide accurate real-time isolation for the fault occurring in the robot. The proposed methods have been validated with physical experiments. In future work, we expect to extend our proposed fault detection and isolation approaches to develop a fault-tolerant control scheme for soft robots.

## REFERENCES

- [1] D. Trivedi, C. D. Rahn, W. M. Kier, and I. D. Walker, "Soft robotics: Biological inspiration, state of the art, and future research," *Applied bionics and biomechanics*, vol. 5, no. 3, pp. 99–117, 2008.
- [2] T. George Thuruthel, Y. Ansari, E. Falotico, and C. Laschi, "Control strategies for soft robotic manipulators: A survey," *Soft robotics*, vol. 5, no. 2, pp. 149–163, 2018.
- [3] Z. Gao, C. Cecati, and S. X. Ding, "A survey of fault diagnosis and fault-tolerant techniques—part i: Fault diagnosis with model-based and signal-based approaches," *IEEE transactions on industrial electronics*, vol. 62, no. 6, pp. 3757–3767, 2015.
- [4] J. Zhang, X. Chen, P. Stegagno, and C. Yuan, "Nonlinear dynamics modeling and fault detection for a soft trunk robot: An adaptive nnbased approach," *IEEE Robotics and Automation Letters*, 2022.
- [5] J. Zhang, Q. Gao, C. Yuan, W. Zeng, S.-L. Dai, and C. Wang, "Similar fault isolation of discrete-time nonlinear uncertain systems: An adaptive threshold based approach," *IEEE Access*, vol. 8, pp. 80755–80770, 2020.
- [6] H. Gu, H. Hu, H. Wang, and W. Chen, "Soft manipulator fault detection and identification using anc-based lstm," in 2021 IEEE/RSJ International Conference on Intelligent Robots and Systems (IROS). IEEE, pp. 1702–1707.
- [7] D. Bruder, X. Fu, R. B. Gillespie, C. D. Remy, and R. Vasudevan, "Koopman-based control of a soft continuum manipulator under variable loading conditions," *IEEE Robotics and Automation Letters*, vol. 6, no. 4, pp. 6852–6859, 2021.
- [8] H. Gu, H. Wang, F. Xu, Z. Liu, and W. Chen, "Active fault detection of soft manipulator in visual servoing," *IEEE Transactions on Industrial Electronics*, 2020.
- [9] H. Gu, H. Wang, and W. Chen, "Toward state-unsaturation guaranteed fault detection method in visual servoing of soft robot manipulators," in 2021 IEEE/RSJ International Conference on Intelligent Robots and Systems (IROS). IEEE, pp. 3942–3947.

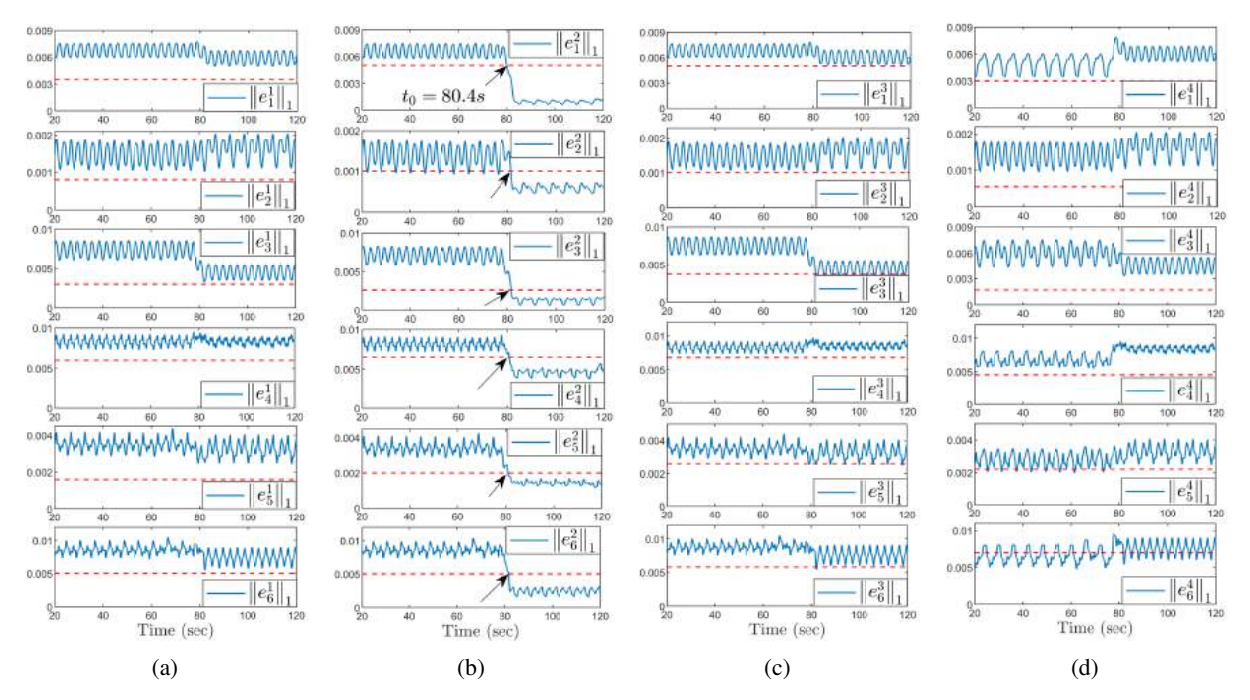


Fig. 5: FI performances of the FI observers (12) for the soft robot in Fig. 1: (a) the 1-st FI observer; (b) the 2-nd FI observer; (c) the 3-rd FI observer; and (d) the 4-th FI observer, where the red dash lines are the corresponding FI thresholds. The fault 2 occurs at time  $t_c = 77.1$  sec and is isolated at time  $t_0 = 80.4$  sec, with the absolute FI time being  $t_0 - t_c = 3.3$  sec.

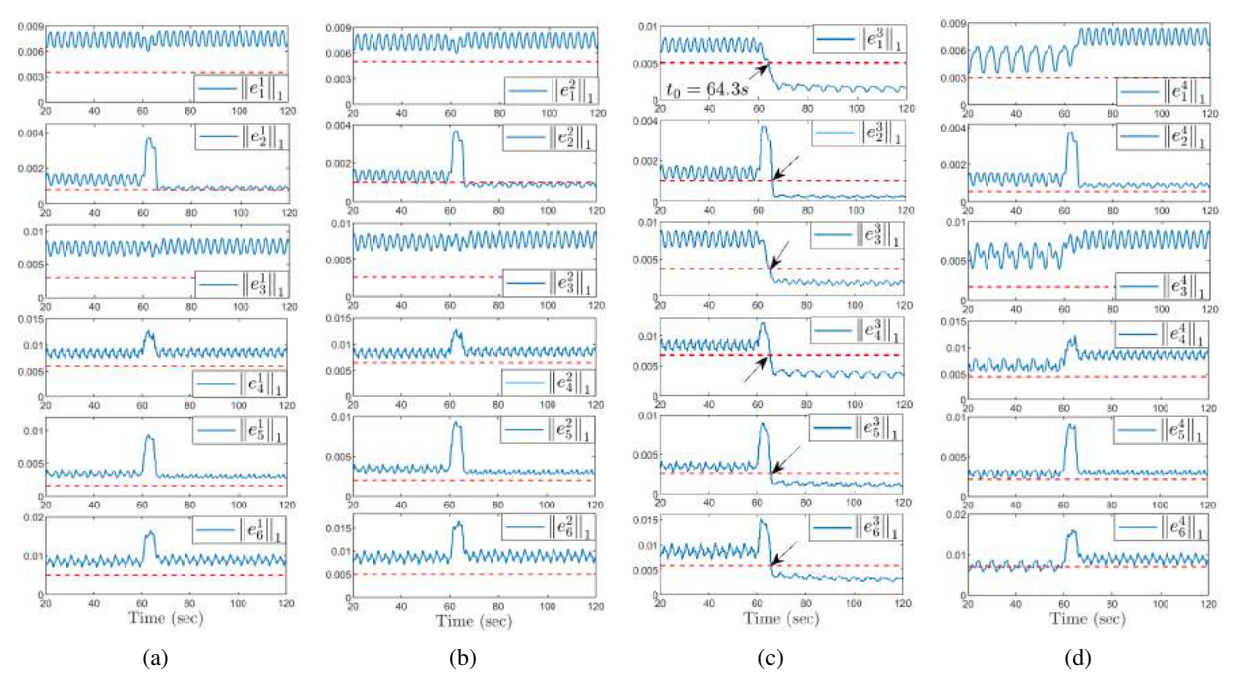


Fig. 6: FI performance of the FI observers (12) for the soft robot in Fig. 1: (a) the 1-st FI observer; (b) the 2-nd FI observer; (c) the 3-rd FI observer; and (d) the 4-th FI observer, where the red dash lines are the corresponding FI thresholds. The fault 3 occurs at time  $t_c = 59.9$  sec and is isolated at time  $t_0 = 64.3$  sec, with the absolute FI time being  $t_0 - t_c = 4.4$  sec.

- [10] C. Wang and D. J. Hill, Deterministic learning theory for identification, recognition, and control. Boca Raton, FL, USA: CRC Press, 2009.
- [11] T. Chen, C. Wang, and D. J. Hill, "Rapid oscillation fault detection and isolation for distributed systems via deterministic learning," *IEEE Transactions on Neural Networks and Learning Systems*, vol. 25, no. 6, pp. 1187–1199, 2013.
- [12] P. Benner, M. Ohlberger, A. Cohen, and K. Willcox, *Model reduction and approximation: theory and algorithms*. Society for Industrial and Applied Mathematics, 2017.
- [13] J. Zhang, C. Yuan, P. Stegagno, and W. Zeng, "Fault isolation of a class of uncertain nonlinear parabolic pde systems," in *Modeling, Estimation* and Control Conference, 2022, to be presented.